ELSEVIER

Clinical Neurophysiology 117 (2006) 912–927

www.elsevier.com/locate/clinph

A system for automatic artifact removal in ictal scalp EEG based on independent component analysis and Bayesian classification

P. LeVan *, E. Urrestarazu, J. Gotman

Montreal Neurological Institute, McGill University, 3801 University Street, Montreal, Que., Canada H3A 2B4

Accepted 13 December 2005
Available online 2 February 2006

Abstract

Objective: To devise an automated system to remove artifacts from ictal scalp EEG, using independent component analysis (ICA).

Methods: A Bayesian classifier was used to determine the probability that 2 s epochs of seizure segments decomposed by ICA represented EEG activity, as opposed to artifact. The classifier was trained using numerous statistical, spectral, and spatial features. The system's performance was then assessed using separate validation data.

Results: The classifier identified epochs representing EEG activity in the validation dataset with a sensitivity of 82.4% and a specificity of 83.3%. An ICA component was considered to represent EEG activity if the sum of the probabilities that its epochs represented EEG exceeded a threshold predetermined using the training data. Otherwise, the component represented artifact. Using this threshold on the validation set, the identification of EEG components was performed with a sensitivity of 87.6% and a specificity of 70.2%. Most misclassified components were a mixture of EEG and artifactual activity.

Conclusions: The automated system successfully rejected a good proportion of artifactual components extracted by ICA, while preserving almost all EEG components. The misclassification rate was comparable to the variability observed in human classification.

Significance: Current ICA methods of artifact removal require a tedious visual classification of the components. The proposed system automates this process and removes simultaneously multiple types of artifacts.

Keywords: EEG; Seizure; Artifacts; Automatic; Independent component analysis; Bayesian classifiers

1. Introduction

Electroencephalogram (EEG) recordings constitute a well-established modality in the diagnosis of epilepsy. The ictal scalp EEG is used to analyze and localize epileptic seizures, thus providing valuable guidance when planning for a potential surgery. Unfortunately, the EEG is frequently contaminated by artifacts originating from various sources such as scalp muscles, eye blinks, eye movements, or patient movement (Niedermeyer and Lopes da Silva, 2005). By obscuring the EEG at the time of seizure onset, these artifacts can greatly hinder the interpretation of the recorded seizures.

Recently, Independent Component Analysis (ICA) has been applied to decompose EEG signals into maximally independent components. This approach has been used to successfully separate and remove artifactual sources from ictal scalp EEG, thus improving the quality of the recordings and facilitating seizure interpretation (Nam et al., 2002; Urrestarazu et al., 2004). However, these methods require the intervention of a trained electroencephalographer to visually inspect the components extracted by ICA and identify those corresponding to artifactual sources. A few software tools have been developed in an attempt to facilitate this time-consuming process by detecting components with unusual statistical properties, with applications to both EEG and magnetoencephalography (MEG) (Barbati et al., 2004; Delorme et al., 2001). However,

* Corresponding author. Address: EEG Department, Room 786, Montreal Neurological Institute, McGill University, 3801 University Street, Montreal, Que., Canada, H3A 2B4. Tel.: +1 514 398 2479; fax: +1 514 398 8106

E-mail address: pierre.levan@mail.mcgill.ca (P. LeVan).

1388-2457/$30.00
doi:10.1016/j.clinph.2005.12.013

these semi-automatic methods still require the manual intervention of users to identify components that were not properly detected by the system. Another approach consists of selecting components highly correlated with a reference signal such as the electro-oculogram (EOG) (Park et al., 2003). Recently, an extension of ICA has also been developed to specifically extract individual components highly correlated with a given reference (James and Gibson, 2003; Lu and Rajapakse, 2005). These methods can be very effective to remove particular artifacts for which a reference signal can be measured. However, an EOG is not always recorded simultaneously with the EEG. Also, many other types of artifactual sources cannot be measured separately to serve as a reference. In that case, other features must be extracted to recognize artifactual components. A lot of research has focused on the automatic recognition of ocular artifacts extracted by ICA using a combination of spectral features, spatial topography, and time-domain signal morphology (Delsanto et al., 2003; Romero et al., 2004). However, these approaches are specific to ocular artifacts and cannot be easily extended to other unwanted signals.

The system described here is an attempt to fully automate the process of artifact removal from ictal scalp EEG based on ICA. Temporal and spatial features were used in a Bayesian classifier to determine whether ICA components represent EEG activity or artifactual signals. Successful classification is crucial not only to remove artifactual components, but also to ensure that components representing EEG activity are preserved. It would then be possible to process ictal scalp EEG without the need for human intervention in identifying artifactual components. While the same methodology could be used on general EEG signals, only ictal recordings were considered here because of their particular importance in clinical applications.

2. Methods

2.1. Data selection

Scalp EEG recordings of 205 seizures from 46 epileptic patients were collected at the Montreal Neurological Institute using the Stellate Harmonie system (Stellate, Montreal, Que., Canada), between December 2000 and February 2004. Patients were only selected if at least two seizures were recorded on the EEG. There was no pre-selection with respect to the amount of artifacts that were present. The seizures did not have to be accompanied by clinical symptoms, but they all had to show visible changes on the EEG signal. The resulting dataset included a wide variety of seizures; 35 patients had focal seizures, while 11 patients suffered from generalized epilepsy. Each patient had between 21 and 39 electrodes with a common reference at FCz. The recorded signals were sampled at 200 Hz after filtering between 0.5 and 70 Hz and were then re-referenced into an average montage. While the montage does not affect the results of ICA, a referential montage was used to allow the generation of topographic maps of the scalp potentials.

2.2. Artifact separation using independent component analysis

For each seizure, a 30 s window was selected starting approximately 10 s before the time of the visually identified seizure onset, thus including a good portion of the seizure activity. Restricting the window length to 30 s limited the number of distinct transient artifactual sources that could be present in the data segment. The FastICA algorithm (Hyvarinen and Oja, 1997) was applied to these seizure segments, using the EEGLAB platform (Delorme and Makeig, 2004) running on MATLAB (The Mathworks, Natick, Massachusetts). The use of other ICA algorithms such as Extended Infomax (Lee et al., 1999) yielded similar source separation results, but FastICA was chosen because its fixed-point method produced faster convergence. The algorithm extracted statistically independent components whose linear mixture could be used to reconstruct the original EEG signal. The number of extracted components was equal to the number of recording electrodes. Each 30 s component was then partitioned into fifteen 2 s epochs. This partitioning was necessary because some components were a mixture of cerebral and artifactual activity, as will be described further below. Using visual inspection of both the time-domain signal and the spatial topography associated with each component, the epochs were classified as representing either EEG or artifactual activity. The small duration of each epoch ensured that this visual classification was generally unambiguous.

Ocular artifacts were easily identified due to the characteristic low-frequency waveforms caused by either eye blinks or eye saccades (Iwasaki et al., 2005). Moreover, the consistent spatial topographies of these artifacts provided another distinguishing factor: eye blinks and vertical eye movements mostly affected fronto-polar electrodes, while horizontal eye movement artifacts were especially present in the F7-F9-F8-F10 electrodes, with a phase reversal between the right and left sides. Patient movement artifacts were characterized by high-amplitude slow waves; these occurred frequently when the patients were changing positions during clinical seizures. Electrode artifacts, due to defective electrodes or faulty connections, could also be clearly identified; they affected only a single electrode and were characterized by either an unusually high amplitude signal or significant power at the mains frequency of 60 Hz. Another very common artifact was caused by the EMG (electromyogram) signal from scalp muscle contractions being recorded by the EEG electrodes. This artifact significantly affects the EEG due to its broad spectrum showing energy at all frequencies from 0 to 200 Hz (Goncharova et al., 2003). In particular, the EMG spectrum overlaps with the ictal EEG, whose energy is mainly contained in the frequencies between 3 and 29 Hz

(Gotman et al., 1981). Epochs contaminated by EMG could be distinguished from EEG epochs by the significant high-frequency activity above 30 Hz. Moreover, since the EMG sources are situated just below the scalp, they do not suffer from the spatial smearing of EEG sources due to their distance from the recording surface and the volume conduction through the highly resistive skull (Srinivasan et al., 1998). Therefore, EMG epochs extracted by ICA were also characterized by a very limited spatial extent. Finally, electrocardiogram (EKG) artifact was also identified as regular spikes time-locked to a reference EKG signal.

ICA-based methods of EEG artifact removal rely on the elimination or preservation of entire components extracted by the algorithm. However, some components were a mixture of both EEG and artifactual segments. To train an automated system to recognize artifacts, it was thus necessary to partition the components into smaller epochs. After manually classifying the 2 s epochs as either EEG or artifact, the entire components themselves were also marked to be either rejected or preserved. Whenever a component was composed entirely of EEG epochs or artifactual epochs, it was clear that the component should be kept or removed, respectively. On the other hand, in the case of a mixture of both types of epochs, components were rejected whenever they would result in no significant EEG activity being removed from the seizure record. In particular, the EEG activity related to the seizure should not be affected by the rejection of a component. This assessment was based on the reviewer's subjective judgment, by comparing the original seizure record with the EEG reconstructed from the component being examined. Therefore, not every artifactual activity could be removed from the recording, since this would have resulted in the loss of EEG activity as well.

2.3. Training of an automated artifact rejection system

2.3.1. Feature extraction

Half of the patients were randomly selected to train the automated system (98 seizures from 23 patients), while the remaining data were reserved for use as a validation set (107 seizures from 23 patients). Features were then computed from the 2 s epochs in each component extracted by ICA.

The relative power in several frequency bands (0–1 Hz, 1–3 Hz, 3–15 Hz, 15–30 Hz, and 30–55 Hz) was calculated from the power spectrum of the epoch, computed with Welch's method using eight 50%-overlapping Hamming windows. Significant power at low frequencies might suggest the presence of ocular or movement artifacts, while the power in the high-frequency band would indicate EMG contamination. In contrast, the middle frequencies would characterize mainly seizure activity. Relative power in the band between 59 and 61 Hz was also calculated to detect the presence of 60 Hz line noise.

The entropy of the power spectrum between 5 and 30 Hz was computed to determine if the epoch had any spectral peaks. This would thus serve as a measure of rhythmicity in the signal (Inouye et al., 1991), which is typical of many seizure patterns. A lower bound of 5 Hz was chosen to avoid interference by ocular artifacts, which can also appear as a peak in the power spectrum.

Statistical properties of the time-domain signal were extracted as well. While ICA components can only be determined up to a scaling factor, it is still possible to reconstruct the EEG from each component to obtain amplitude information. The total variance of each epoch was thus calculated across all channels in the reconstructed EEG. Abnormally large values would probably reflect artifactual activity such as electrode artifacts. The negentropy of the component was also computed as a measure of the randomness of the time-domain signal with respect to a Gaussian-distributed signal with the same variance. This measure was calculated using the same robust approximation used in the FastICA algorithm (Hyvarinen and Oja, 2000)

$$J(y) \propto [E\{G(y)\} - E\{G(\mu)\}]^2$$

where $J(y)$ is the negentropy of the zero mean and unit variance variable y, $E\{\cdot\}$ denotes the expected value, μ is a Gaussian random variable of zero mean and unit variance, and G is the contrast function $\log(\cosh(\cdot))$.

In many cases, the amplitude distribution of artifactual activity will tend to have many outliers, which would be reflected in its negentropy. This property was calculated for the entire component, rather than individual epochs, to ensure that enough data points were used to get an accurate estimate of the amplitude distribution of the signal.

ICA components were also characterized by a spatial topography corresponding to the contribution of each electrode to the linear mixture. Since each ICA component is generally assumed to represent a single independent source, this spatial information is often modelled by an equivalent current dipole. For this purpose, a standard 4-shell spherical model of the head was used to represent brain, cerebrospinal fluid, skull, and scalp layers. Whenever the residual variance of the fitted model was less than 20%, the position of the resulting dipole in the *xyz*-space was used as a feature in the system, along with its eccentricity, namely the distance from the dipole to the center of the spherical model. Ocular artifacts were thus characterized by a dipole position at the front of the head, while dipoles corresponding to EMG activity were mostly near the head surface. On the other hand, components representing seizure activity should result in dipoles inside the brain layer of the head model. The use of a single point dipole in an approximate head model is inaccurate, but the objective was only to obtain sufficient localization information to distinguish between artifacts and EEG activity (Flanagan et al., 2003).

EKG artifacts could be detected by calculating the correlation of the ICA components with a reference EKG signal, which is usually recorded simultaneously with the

EEG. However, EKG artifacts almost never occurred in the dataset, so no attempt was made to detect them.

2.3.2. Bayesian network classification

The extracted features were then used to train a classifier to distinguish between EEG and artifactual epochs. The chosen approach relies on Bayes' theorem to compute the probability that an epoch represents EEG activity:

$$P(\text{EEG}|\text{features}) = \frac{P(\text{features}|\text{EEG})P(\text{EEG})}{P(\text{features})}$$

The term $P(\text{EEG}|\text{features})$ is the posterior probability that an epoch represents EEG activity, given the calculated features. The terms on the right-hand side of the equation can be estimated from the manual classification of the training data. The term $P(\text{EEG})$ is the prior probability that any given epoch represents EEG activity, and not artifact. $P(\text{features}|\text{EEG})$ is the likelihood that the calculated features will be observed in EEG epochs. $P(\text{features})$ is a normalizing constant representing the probability that the given features will be present. A similar equation can be used to calculate the probability that an epoch represents artifactual activity:

$$P(\text{artifact}|\text{features}) = \frac{P(\text{features}|\text{artifact})P(\text{artifact})}{P(\text{features})}$$

Because of the large number of features, the likelihood terms $P(\text{features}|\text{EEG})$ and $P(\text{features}|\text{artifact})$ represent highly-dimensional probability density functions (PDFs). A probability would need to be computed for every possible combination of values of each feature. This could be accomplished by dividing each feature into, say, 10 discrete bins. There would then have to be enough data belonging to each possible combination of bins to estimate the required probability. However, with 13 features, there would be a total of 10^{13} different combinations of bins; the amount of data required to estimate the PDFs accurately is thus impractical.

Therefore, the PDFs were modelled using tree-augmented naïve (TAN) Bayesian networks (Friedman et al., 1997). Bayesian networks are directed acyclic graphs where each vertex is associated with either a feature or the class attribute (EEG or artifact). Edges join any variables that are directly correlated, and an attribute is considered to be conditionally independent of its non-descendants, given the state of its parents. The Bayesian network encodes the joint PDF of all of its attributes, which can be calculated using the following formula (Friedman et al., 1997)

$$P(X_1, X_2, \ldots, X_n) = \prod_{i=1}^{n} P(X_i|\prod\nolimits_{X_i})$$

where the product is over all the attributes X_i, and $\prod_{X_i}$ denotes the parents of X_i.

The TAN model starts by falsely assuming that all features are statistically independent, given the classification of the epoch as either EEG or artifact. In this so-called naïve approach, the corresponding Bayesian network has edges going from the class variable to each feature, and the global PDF would then be the product of the marginal PDFs of each feature, given the class variable. Since the independence assumption is unrealistic, TAN Bayesian networks extend the naïve method by characterizing some of the strongest dependencies between the various features. These dependencies are determined by computing the conditional mutual information between all pairs of features, given the class attribute (Friedman et al., 1997)

$$I(X; Y|C) = \sum_{x,y,c} P(x, y, c)\log\frac{P(x, y|c)}{P(x|c)P(y|c)},$$

where X and Y are two features and C denotes the class attribute.

A maximum spanning tree can then be constructed based on these mutual information values, using standard greedy algorithms (Cormen et al., 1990). Edges belonging to this spanning tree are added to the Bayesian network to yield the TAN model. Since these additional edges form a tree structure, each variable in the resulting Bayesian network will have as parents the class attribute and at most one other feature. The likelihood terms are thus still expressed as products of several low dimensional PDFs, which can be estimated using the available training data. It should also be noted that, as described previously, the set of features depended on whether the spatial topography of a component could be fitted with a dipole with less than 20% residual variance. Two separate Bayesian networks were thus constructed for both dipolar and non-dipolar components.

2.3.3. Feature discretization

In order to estimate the PDFs of the various features, histograms were computed by discretizing the continuous-valued features into several bins. The cutoff points between successive bins were determined based on the method of Fayyad and Irani (Fayyad and Irani, 1993). For a given dataset, its class entropy is defined as:

$$\begin{aligned}\text{Entropy} = &-P(\text{EEG})\log(P(\text{EEG})) \\ &- P(\text{artifact})\log(P(\text{artifact}))\end{aligned}$$

This measure is minimized whenever the subset contains elements belonging to a single class, either EEG or artifact. The optimal cutoff point to partition a set S into two subsets S_1 and S_2 was then chosen to minimize the class entropy of each subset, weighted by their respective size:

$$\text{Minimize}\,\frac{|S_1|}{|S|}\text{Entropy}(S_1) + \frac{|S_2|}{|S|}\text{Entropy}(S_2)$$

The optimal cutoff point thus ensures that the classification values for each bin are as homogeneous as possible. The procedure is repeated recursively on the two resulting partitions to yield a finer discretization. The minimum description length (MDL) principle was used to determine

when to stop partitioning the data further (Fayyad and Irani, 1993). This specified that the information gain due to a new cutoff point should be greater than the cost of coding the additional partitions. The information gain is equal to the difference between the class entropy of the original set S and that of the partitions S_1 and S_2:

$$\text{Gain} = \text{Entropy}(S) - \frac{|S_1|}{|S|}\text{Entropy}(S_1) - \frac{|S_2|}{|S|}\text{Entropy}(S_2)$$

Also, it can be shown (Fayyad and Irani, 1993) that the cost of coding the resulting partitions is given by:

$$\text{Cost} = \frac{\log_2(|S|-1)}{|S|} + \frac{\log_2(3^k-2)}{|S|} - \frac{k\text{Entropy}(S) - k_1\text{Entropy}(S_1) - k_2\text{Entropy}(S_2)}{|S|},$$

where k is the number of classes in the original set S, and k_1 and k_2 are the number of classes represented in the two resulting subsets S_1 and S_2. In this formula, the first term is related to coding the cutoff point, the second term accounts for the specification of the classes in each subset, and the third term computes the cost difference between coding the classes in the original set and in the partitions.

While the MDL principle ensures that any new partition will provide a better separation between the two classes of EEG and artifact, the resulting discretization might produce very small bins containing very little data. This could lead to inaccurate estimations of the probabilities required for the Bayesian classification task. To prevent this overfitting phenomenon, an additional criterion was that each bin had to contain at least 5% of the data. Using the specified cutoff thresholds, it was then possible to induce a TAN Bayesian network classifier to distinguish between EEG and artifactual epochs.

2.3.4. Component classification

The output of the classifier was the probability that a 2 s epoch from an ICA component represented EEG activity. Based on the classification of the 15 epochs in a 30 s ICA component, the system then had to determine whether the component should be rejected or preserved. For this purpose, a threshold on the number of epochs being classified as EEG was used; components whose number of EEG epochs was below the threshold were rejected. Since the Bayesian classifier only returns a probability that an epoch represents EEG activity, the system used the sum of the probabilities for all epochs. The value of the threshold was selected so that at least 90% of EEG components would be correctly identified in the training data. The system was then applied on the previously unseen validation set to determine its classification accuracy.

2.3.5. Analysis of reconstructed seizure records

An expert neurologist was asked to review the performance of the system. The reviewer carried out a subjective evaluation based on several criteria (Table 1) by examining the original EEG records and the EEGs reconstructed after rejecting artifactual components in the validation dataset. These two records had to be reviewed simultaneously, as it would otherwise be impossible to evaluate whether the system inadvertently removed cerebral activity from the recording.

The neurologist estimated the amount of artifacts present in the original EEG as a measure of the record quality. Using the designations in table 1, the reviewer indicated 'almost none' when the amount of visually identified artifacts was negligible while the designation 'few' was used when artifacts were detected, but did not significantly obscure the EEG activity. The other categories ('significant' and 'considerable') implied a substantial amount of artifacts that greatly affected the EEG. In particular, the category 'considerable' was reserved for cases where high-amplitude artifacts were present for a long period of time and affected multiple channels.

The amount of artifacts in the EEG reconstructed after processing by the automated system was evaluated relative to the original record. A score of 'mostly removed' meant that almost no artifactual activity remained in the processed EEG. Indications of 'major improvement' and 'minor improvement' denoted various degrees of artifact removal. The artifact removal was considered to result in an improvement if it became easier to see the EEG activity that was previously obscured. Otherwise, the score 'similar or worse' was given. It should be noted that the automated system was not expected to worsen the amount of artifacts, but this was still included for completeness.

The system was designed to remove artifactual activity from ictal recordings, but it was even more important that all cerebral activity from the original EEG be preserved in the processed EEG. The reviewer thus compared the EEG activity in the two records simultaneously. A 'major attenuation' was indicated when some significant EEG activity disappeared or was significantly attenuated in the processed record. If some EEG activity was attenuated, but was still clearly visible despite a slightly reduced amplitude, then a 'minor attenuation' was noted. A score of 'mostly preserved' denoted that all significant EEG activity was preserved. There might have been some small attenuation of background EEG, but all seizure EEG still had to be present. Finally, the category 'all preserved' was reserved for cases

Table 1
Scoring categories for each review parameter

Artifacts in the original record	Considerable	Significant	Few	Almost none
Artifacts removal	Similar or worse	Minor improvement	Major improvement	Mostly removed
EEG removal	Major attenuation	Minor attenuation	Mostly preserved	All preserved

where all the EEG visible in the original record was left intact by the automated system.

3. Results

All reported global statistics were first computed on individual seizures. The records from each patient were then averaged to yield statistics for individual patients. Global results were then obtained by further averaging the results from each patient. This approach was necessary to remove any bias caused by patients having different numbers of recorded seizures and, in the case of one patient, having a different number of electrodes between recording sessions.

3.1. Manual classification by visual inspection

For the training set, manual classification of epochs as either EEG or artifact yielded, on average, 7.4 epochs representing EEG activity, out of a possible 15 epochs per component. The contamination of seizures by artifactual activity varied greatly from patient to patient, as the average number of EEG epochs per component was as low as 2.3 for one patient and as high as 13.2 for another patient. As for the validation set, the average number of EEG epochs ranged from 3.0 to 11.3, for a global average of 7.5. The average proportion of ICA components that were preserved for each patient in the training set varied from 36.5 to 90.4%, for a global average of 62.2%. In the validation set, the proportion ranged from 34.6 to 88.5%, for a global average of 64.6%.

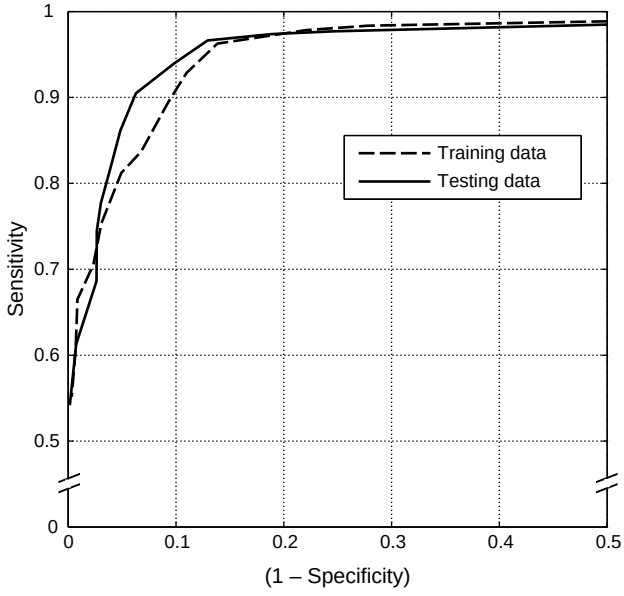

Fig. 1. ROC curves showing the sensitivity and specificity to EEG components for the full range of thresholds on the number of EEG epochs in the components. The results are based on the manual classification of epochs and components by the reviewer. Dotted line, ROC curve for the training data. Solid line, ROC curve for the testing data.

To determine whether a component should be rejected or preserved, a threshold was used on the number of EEG epochs in that component. This approach was first tested on the manually classified data. A Receiver Operating Characteristic (ROC) curve (Metz, 1978) was constructed to represent the classification accuracy for different values of the threshold. As the threshold increases from 0 to 15, the sensitivity to EEG components gradually decreases, while the specificity increases since components below the threshold are now identified as artifact and rejected. For the training set, the area under the ROC curve was 0.966; for the validation set, the area was 0.968 (Fig. 1).

3.2. Automated classification

3.2.1. Bayesian network induction

Examples of the probability distributions of the features are shown in Fig. 2. The distribution for the relative power between 30 and 55 Hz in artifactual epochs show that this

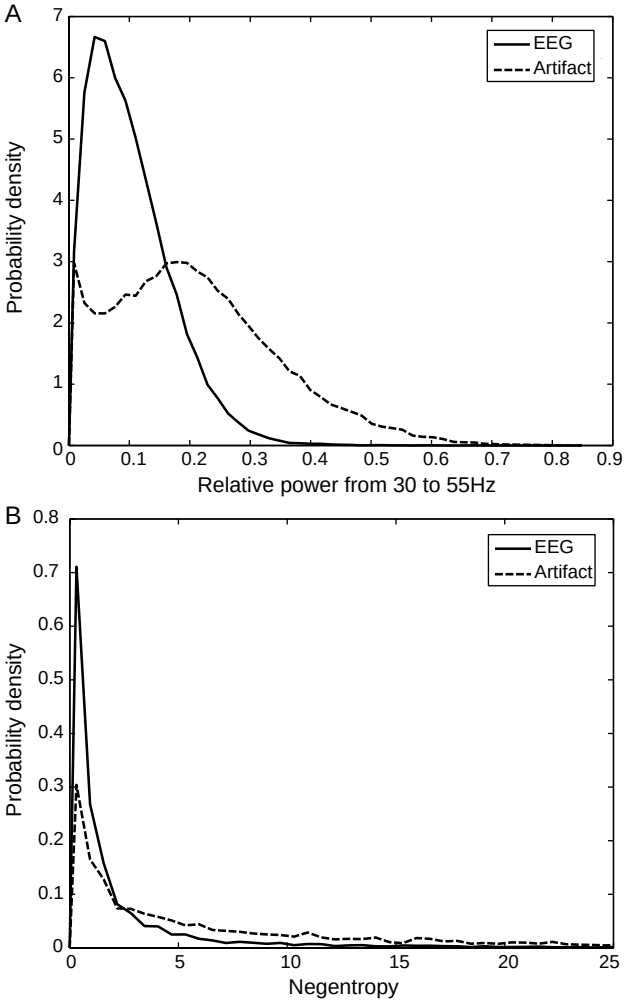

Fig. 2. Examples of probability distribution functions of features for EEG (solid lines) and artifactual (dashed lines) epochs. (A) Probability distribution of the relative power between 30–55 Hz. (B) Probability distribution of the negentropy.

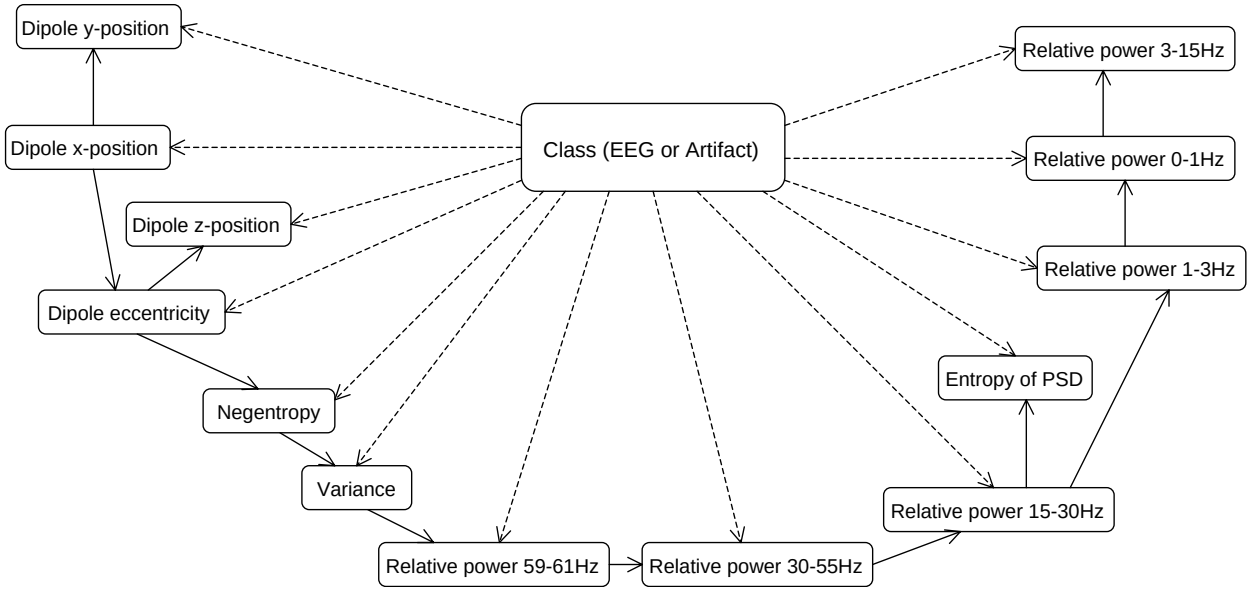

Fig. 3. TAN Bayesian network induced from epochs belonging to dipolar components in the training set. All features are shown as nodes in the graph, in addition to the class attribute, which represents whether the epoch is EEG or artifact. Correlation edges are shown as arrows pointing from parent nodes to child nodes. In TAN Bayesian networks, each feature is a child of the class attribute (dotted lines) and of at most one other feature (solid lines).

feature took values that were either very high, probably due to EMG artifacts, or very low, which would reflect movement and EOG artifacts. On the other hand, for EEG epochs, this feature took values mostly between these two extremes. As for the negentropy feature, the probability distribution of artifactual epochs has a much heavier tail than that of EEG epochs. This probably reflects transient activity such as movement artifact, whose distribution is highly non-Gaussian and thus has a high negentropy value. The different distributions of the features between EEG and artifactual epochs allowed them to be used in the Bayesian classifiers to separate the two types of epochs.

Two TAN Bayesian networks were induced from the training data for components with either a dipolar or non-dipolar spatial topography (Figs. 3 and 4). Every feature in the network is a child node of the class attribute (EEG or artifact) and of at most one other feature, as indicated by the correlation edges in the graph. Because of this restriction, only the strongest dependencies are modelled. Features not linked by an edge are assumed to be independent given the state of their respective parent nodes.

The network corresponding to dipolar components thus shows edges between the dipole parameters of x, y, and z positions, as well as eccentricity. There are also dependencies between the spectral features (relative power in frequency bands, entropy of power spectral density). A correlation was identified between the two amplitude distribution features of negentropy and variance, and also between the variance and the 60 Hz activity (relative power between 59 and 61 Hz).

For non-dipolar components, the induced Bayesian network is almost identical after the removal of the dipole features. The only other difference is that there is no longer a correlation edge between the variance attribute and the

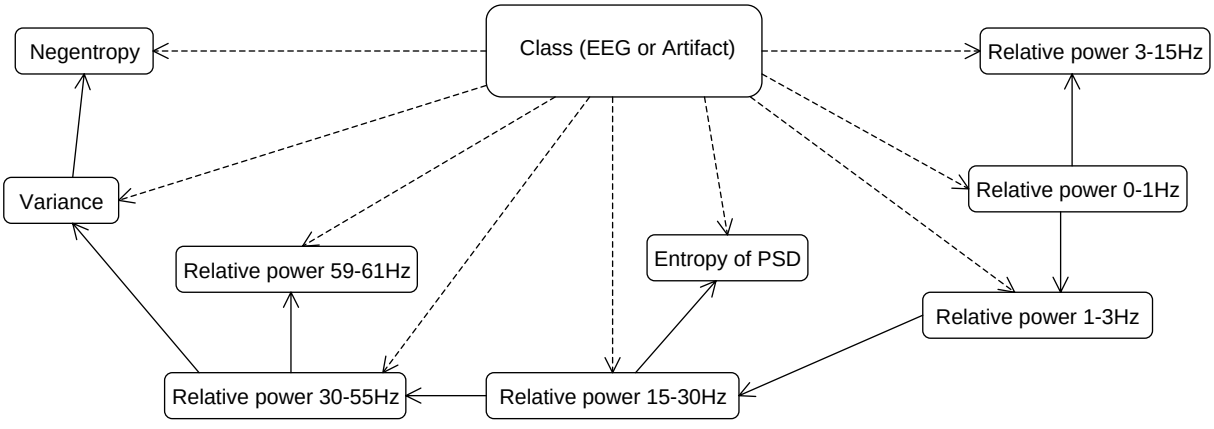

Fig. 4. TAN Bayesian network induced from epochs belonging to non-dipolar components in the training set.

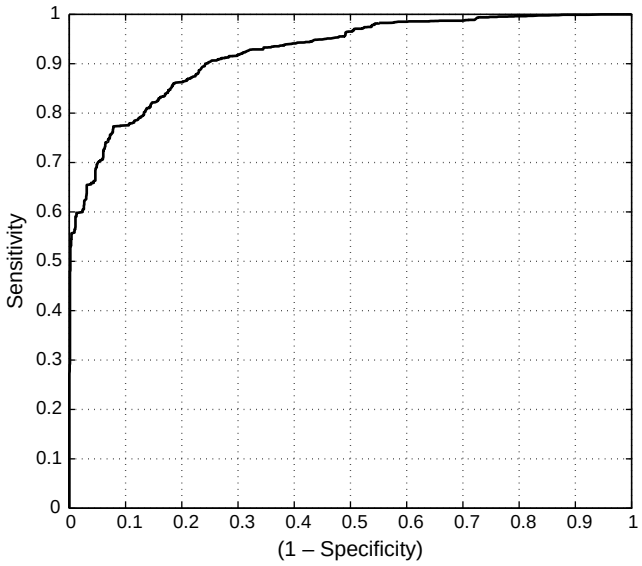

Fig. 5. ROC curve showing the system's performance in classifying components in the training set. For each component, a threshold is used on the sum of the probabilities that the component's epochs represent EEG activity. For the full range of threshold values, the component classification sensitivity and specificity are plotted.

power at 60 Hz. Instead, there is a dependency between the variance and the relative power between 30 and 55 Hz.

It should be noted that among components that were manually classified as EEG in the training set, 64.7% had a dipolar spatial distribution. In the validation set, 57.6% of the EEG components were dipolar. A large number of components were a mixture of cerebral and artifactual activity and had to be marked as EEG. These components were a mixture of several sources and their spatial distribution thus could not be explained by a single equivalent dipole. Because of this significant minority of EEG components that were non-dipolar, it was necessary to have the two separate Bayesian classifiers for the automated classification task.

3.2.2. Classification results

The output of the Bayesian classifier was the probability that the epoch under consideration represented EEG activity. To evaluate the performance of the classifier, an epoch was considered to have been classified as EEG whenever the output probability exceeded 50%. Comparing these results with the manual classification by the reviewer, the system successfully recognized EEG epochs with an average sensitivity of 84.8% and an average specificity of 85.3% in the training data. By using the same classifier on the previously unseen validation set, the average sensitivity was 82.4% and the average specificity was 83.3%.

The sum of the probabilities of epochs representing EEG activity was then used to determine whether to reject or preserve each component. A threshold was selected by constructing a ROC curve based on the classification results on the training data. The sensitivities and specificities were calculated with respect to the manual classification of components that was performed by the reviewer (Fig. 5). The area under the curve was 0.923. The threshold was chosen so that EEG components could be identified with an average sensitivity of 90%. This criterion yielded a threshold of 3.92, which corresponded to an average specificity of 75.8%. This threshold obtained from the training data was then applied to the validation set. EEG components could then be detected with an average sensitivity of 87.6% and an average specificity of 70.2%. In most cases, components contained almost exclusively artifactual epochs or almost exclusively EEG epochs. The automated system had little difficulty in correctly classifying these components, since their sum of probabilities of their epochs was clearly above or below the threshold (Fig. 6).

Most misclassified components were a mixture of both EEG and artifactual activity. Components marked as artifacts by the reviewer, but classified as EEG by the automated system, usually had major artifactual activity with some EEG activity that was not deemed to be significant (Fig. 7A). However, the automated system still detected a sufficient number of EEG epochs to preserve the component. A similar situation occurred with EEG components misclassified as artifact by the system. This time, however, the minor EEG activity was deemed to be significant enough by the reviewer to preserve the component, but the system did not detect a sufficient number of EEG epochs and thus rejected it (Fig. 7B).

3.3. Review of reconstructed seizures

A global summary of the average reviewer scores for the various criteria can be found in Table 2. A majority of seizure records (70.3%) had either a significant or considerable amount of artifacts, while only a small proportion (9.9%) had almost no artifacts. After processing by the automated system of artifact removal, a large proportion of records (44.9%) showed a major improvement in the amount of artifacts, but only in 3.9% of the seizures were the artifacts mostly removed. Despite the persistence of some artifacts, seizure records could still become easier to interpret. Fig. 8 shows a seizure that was heavily contaminated by muscle activity on numerous channels. According to the reviewer, the amount of artifacts was 'considerable'. After the system processed the record, some EMG activity still remained but was greatly attenuated, resulting in a 'major improvement'. Even though the artifacts could not be completely removed, the performance of the system was still sufficient to reveal EEG activity that was previously obscured, resulting in a seizure that was easier to interpret.

There were many cases (25.5%) where the reviewer indicated no improvement in the amount of artifacts,

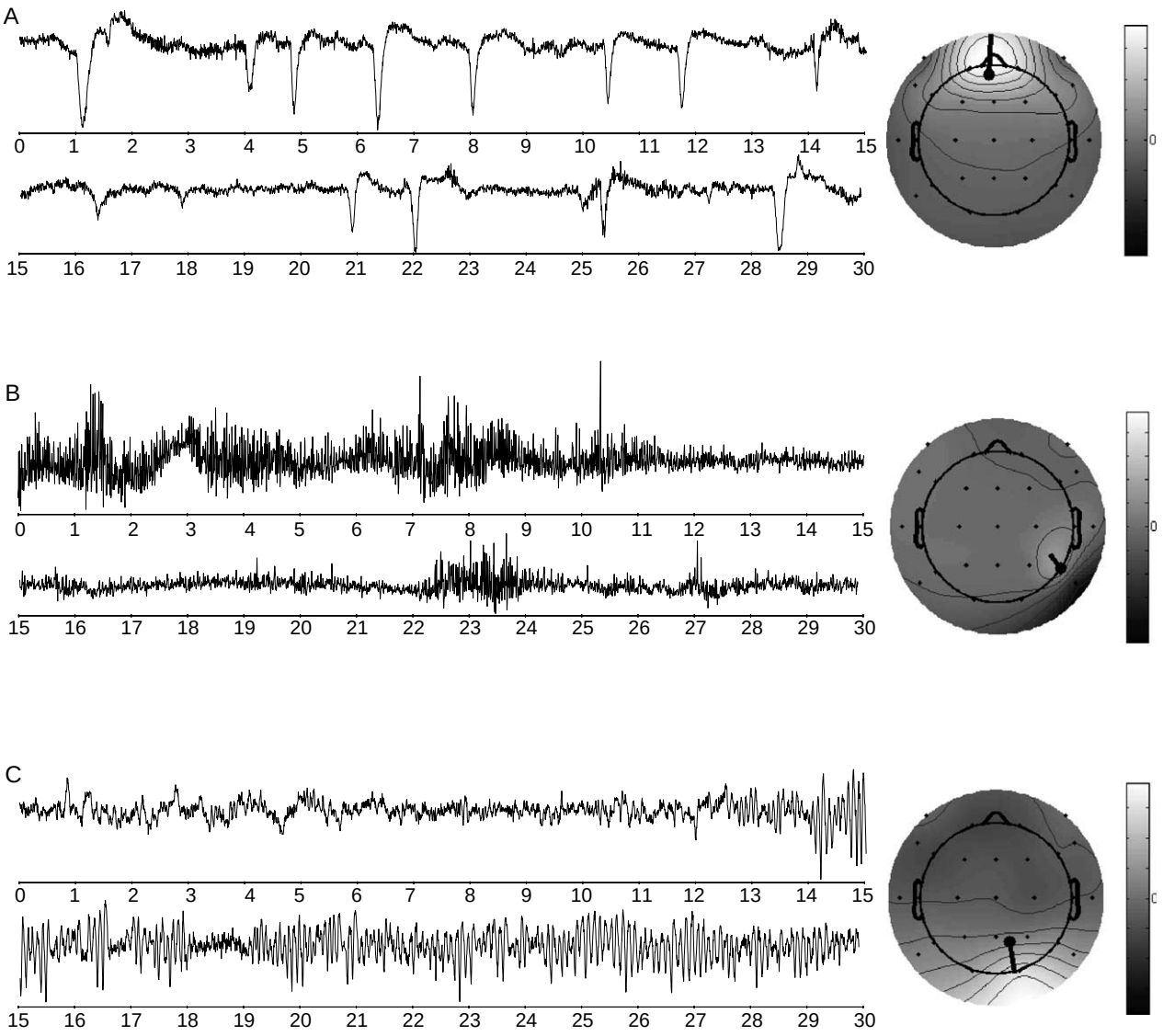

Fig. 6. Components that were easily classified by the automated system. The second line is a continuation of the first. Scalp maps associated to the components and the corresponding dipoles fitted to these spatial distributions are also drawn. (A) Eye blink component classified as artifact. The sum of the probabilities that its 2 s epochs represented EEG activity was only 2.42, which was below the threshold of 3.92. The only epoch with an EEG probability greater than 50% was from 26–28 s, where little ocular activity is visible. (B) EMG component removed by the system. Every epoch yielded an almost-zero probability of representing EEG activity, for a sum of probabilities of 0.001. (C) Seizure component preserved by the system. EEG activity is visible in all epochs, resulting in a sum of probabilities of 14.99, out of a possible 15.

and in an additional 25.8% of records, there was only a minor improvement. It should be noted that these numbers include seizures for which no improvement was possible because the original records did not contain many artifacts to start with. Nevertheless, there were still cases where seizures had a considerable amount of artifacts and where the automated system yielded only a minor improvement, which was not sufficient to improve the ease of interpretation of the seizure. In the example shown in Fig. 9, the EMG artifact has been attenuated slightly, but is still significant in many channels. Movement artifact was largely removed.

Only 4.3% of the seizure records suffered from major EEG attenuation, while in 72.5% of seizures the EEG activity was all preserved. An example of major EEG attenuation is shown in Fig. 10. While the system successfully managed to reduce artifactual activity due to muscle and movement, there were also many channels where EEG activity that was clearly visible in the original record became greatly reduced in amplitude. Nevertheless, most records displayed no EEG attenuation; an example is shown in Fig. 11. This seizure was heavily contaminated by eye blinks, eye movements, and muscle activity. The automated system successfully eliminated most of the artifacts, while preserving all of the EEG activity.

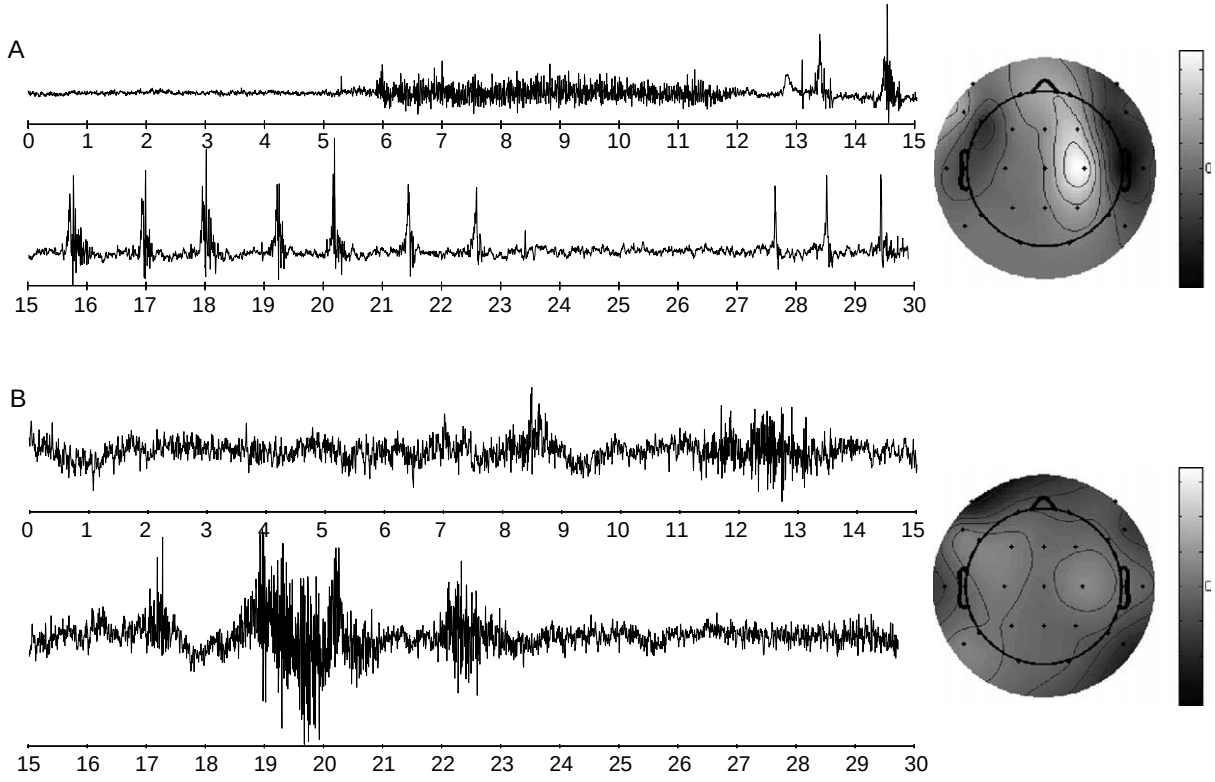

Fig. 7. Components containing a mixture of EEG and artifactual activity. Scalp maps associated to the components are also drawn. In both cases, the spatial distribution could not be fitted with a single equivalent dipole with a residual variance under 20%. (A) Component classified as artifact by the reviewer, but as EEG by the system. EMG activity from 6–12 s and chewing artifact from 13–23 s and 27–30 s are visible. However, EEG seizure activity is also present from 15–30 s. The sum of probabilities of epochs representing EEG activity was 5.32. (B) Component classified as EEG by the reviewer, but as artifact by the automated system. EMG artifact is present from 11–14 s and from 18–23 s, but the reviewer also noted EEG activity from 0–12 s, which was deemed to be significant enough to preserve the component. The sum of probabilities of epochs representing EEG activity was 2.78.

Table 2
Proportion of seizures in each scoring category for all review parameters

Artifacts in the original record	Considerable 21.8%	Significant 48.5%	Few 19.8%	Almost none 9.9%
Artifacts removal	Similar or worse 25.5%	Minor improvement 25.8%	Major improvement 44.9%	Mostly removed 3.9%
EEG removal	Major attenuation 4.3%	Minor attenuation 11.2%	Mostly preserved 12.0%	All preserved 72.5%

4. Discussion

4.1. Artifact separation by ICA

Several methods have been explored in the literature to attempt to remove artifacts from EEG recordings. If a reference signal for an artifact is available, such as the EOG, it can be subtracted from the EEG after scaling it by an appropriate factor determined by regression either in the time domain (Gratton et al., 1983) or frequency domain (Whitton et al., 1978). However, the recorded EOG tends to be contaminated by brain activity as well; regressing it out would thus attenuate the EEG, which is undesirable. Moreover, reference signals are not available for other artifacts such as the EMG. Another approach for artifact elimination is to use digital filters; however, the frequency spectrum of most artifacts overlaps with that of the EEG, hence the artifacts can only be partially removed by this method.

More recently, principal component analysis (PCA) has been used to separate the EEG into uncorrelated components. Artifactual components can be identified and removed, especially if their amplitude is high (Lagerlund et al., 1997). However, PCA restricts the extracted components to have orthogonal spatial topographies, which is an unrealistic assumption (Ille et al., 2002). ICA uses a stronger assumption of statistical independence, which is more appropriate for EEG recordings. It is very difficult, however, to demonstrate that the extracted components correspond to the individual generators of the recorded signal, because the actual time courses of these sources cannot be measured directly. Nevertheless, simulation studies support the use of ICA to separate artificial sources from synthetic EEG signals (Barbati et al., 2004). Equivalent dipoles fitted to sources extracted by ICA have also been shown to match the fields measured by

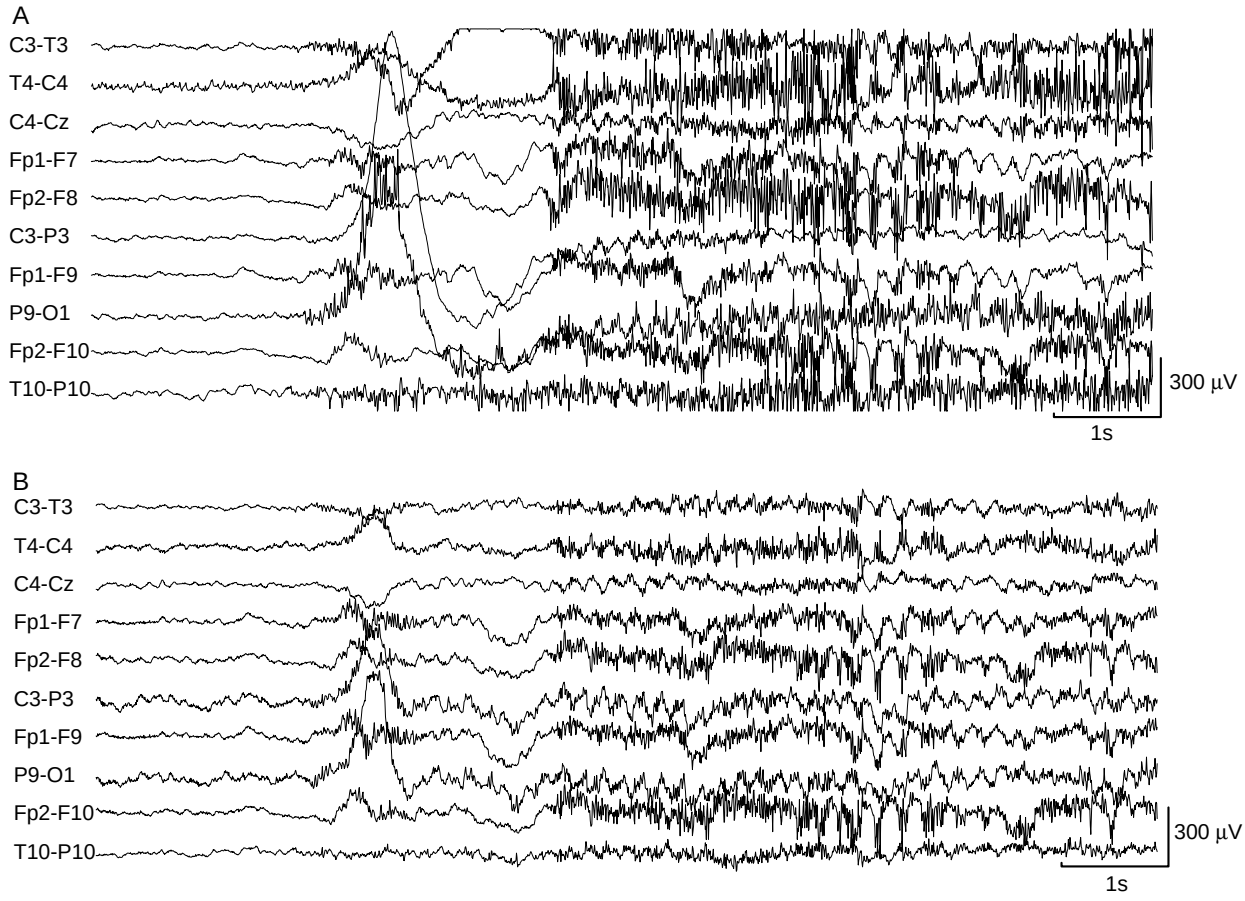

Fig. 8. (A) Seizure heavily contaminated by muscle and movement artifacts in numerous channels. (B) After processing, the artifacts persist, but are greatly attenuated, facilitating interpretation.

intracranial electrodes (Kobayashi et al., 2001). Consequently, ICA applied to scalp EEG was expected to separate artifactual sources into distinct components. However, this separation is usually not ideal because EEG recordings tend to violate one of the fundamental assumptions of ICA, namely that the number of sources should be equal to the number of recording channels (Makeig et al., 1996a). It is impossible to determine the exact number of independent brain signals being recorded on the scalp, in addition to the numerous extra-cerebral sources of noise and artifacts. Nevertheless, it has been shown that ICA tends to separate the strongest sources, while weaker generators are scattered into multiple components (Makeig et al., 1996b). In this case, each ICA component is a mixture of a separated strong source with additional contributions from weaker sources with similar spatial distribution.

However, in the case of EEG heavily contaminated by artifacts, some components might be a mixture of multiple strong sources. The mixture of these strong sources will tend to be normally distributed, which would make the ICA decomposition unpredictable (Hyvarinen et al., 2001). ICA cannot separate sources with a Gaussian distribution; this should thus still allow ICA to isolate sources of rhythmic synchronous epileptic activity, or transient artifactual sources such as the EOG. On the other hand, the EMG signal is the result of the summation of the activity from several asynchronous muscle cells and should thus tend toward a Gaussian distribution. It has indeed been reported that the performance of ICA may degrade when trying to remove EMG artifacts from the EEG (Nam et al., 2002; Urrestarazu et al., 2004). The probability distributions of the negentropy feature shown in Fig. 2 indicate that several components had a negentropy close to zero, which corresponds to Gaussian distributions. These components probably were the result of mixtures of several sources, which might contain both significant EEG and artifactual activity. In this case, artifacts could not be entirely removed since this would have also eliminated EEG activity. Nevertheless, ICA can still successfully isolate components with distributions that deviate only slightly from normality (Jung et al., 2000). The system was thus still able to remove several artifactual components from the seizure recordings.

During the visual inspection of the seizure recordings, the number of identified EEG epochs varied greatly for the various components. There were many instances of components that were not entirely composed of either EEG or artifactual epochs. The decision on whether to preserve or reject these components was left to the

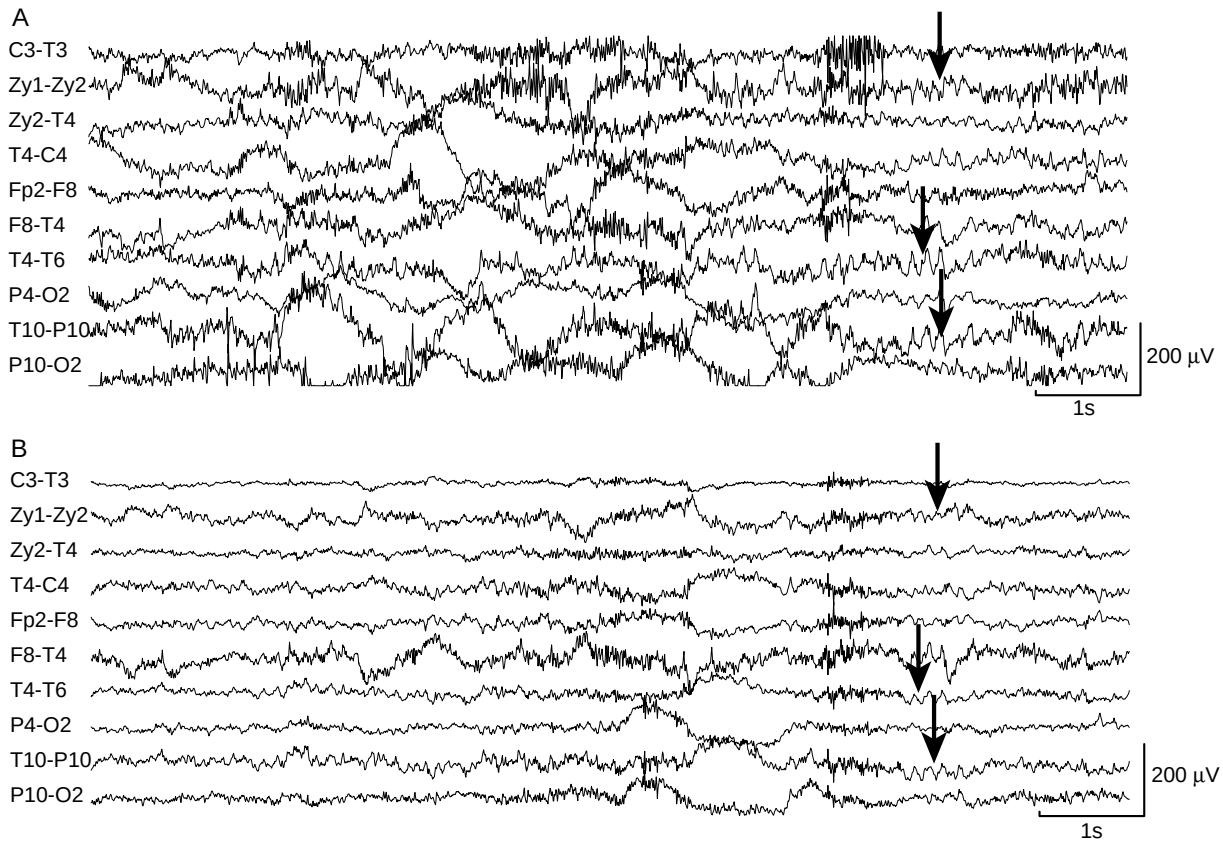

Fig. 9. (A) Seizure with EMG and movement artifacts on numerous channels. (B) Minor improvement in the amount of artifacts. The EMG artifact has been attenuated, notably in channels T4-C4 and Fp1-F3, and movement artefact is largely eliminated. However, large artifacts are still present and the seizure remains difficult to interpret.

subjective judgment of the reviewer. The automated system was thus likely to reflect this; in the future, a more accurate gold standard could be obtained by combining the results from multiple reviewers.

Components were preserved whenever they contained EEG activity that was deemed to be significant. Since ICA components were assumed to represent a mixture of spatially stationary sources, it was unlikely that significant EEG activity would only be present in a few epochs. Using a threshold on the number of EEG epochs should thus be an appropriate criterion to preserve or remove components. This is demonstrated by the constructed ROC curve; the area under the curve was used as a measure of the threshold's discrimination power between EEG and artifactual components (Swets, 1988). For the training set, the area under the ROC curve was 0.966, indicating that a threshold on the number of EEG epochs can provide excellent separation between the two types of components.

4.2. TAN Bayesian classification

The use of a Bayesian formulation to classify EEG signals has previously been applied successfully in seizure detection systems (Grewal and Gotman, 2005; Saab and Gotman, 2005). This framework was refined here by introducing the TAN Bayesian network structure to allow the use of a larger number of features. The induced TAN Bayesian networks show the dependencies that were modelled to estimate the PDFs of the various features. For example, electrode artifacts tended to be associated with both a high variance and activity at 60 Hz. There was thus a correlation edge between those two features, but only for the dipolar case, since electrode artifacts mostly affected a single channel and could therefore be fitted with a dipole at the electrode location. In the non-dipolar case, high amplitude was more likely to be associated with EMG activity, hence the edge between the features of variance and relative power between 30 and 55 Hz. Despite these modelled dependencies, there are also pairs of features that are incorrectly assumed to be independent. In particular, all the features of relative power in various frequency bands are mutually dependent and should therefore have correlation edges between every pair of them. A similar reasoning applies for all features related to dipole position. However, the TAN Bayesian structure restricts the dependencies to ensure that the classification is computationally tractable. Although this will cause inaccuracies in the output probabilities of the system, it has been shown that TAN

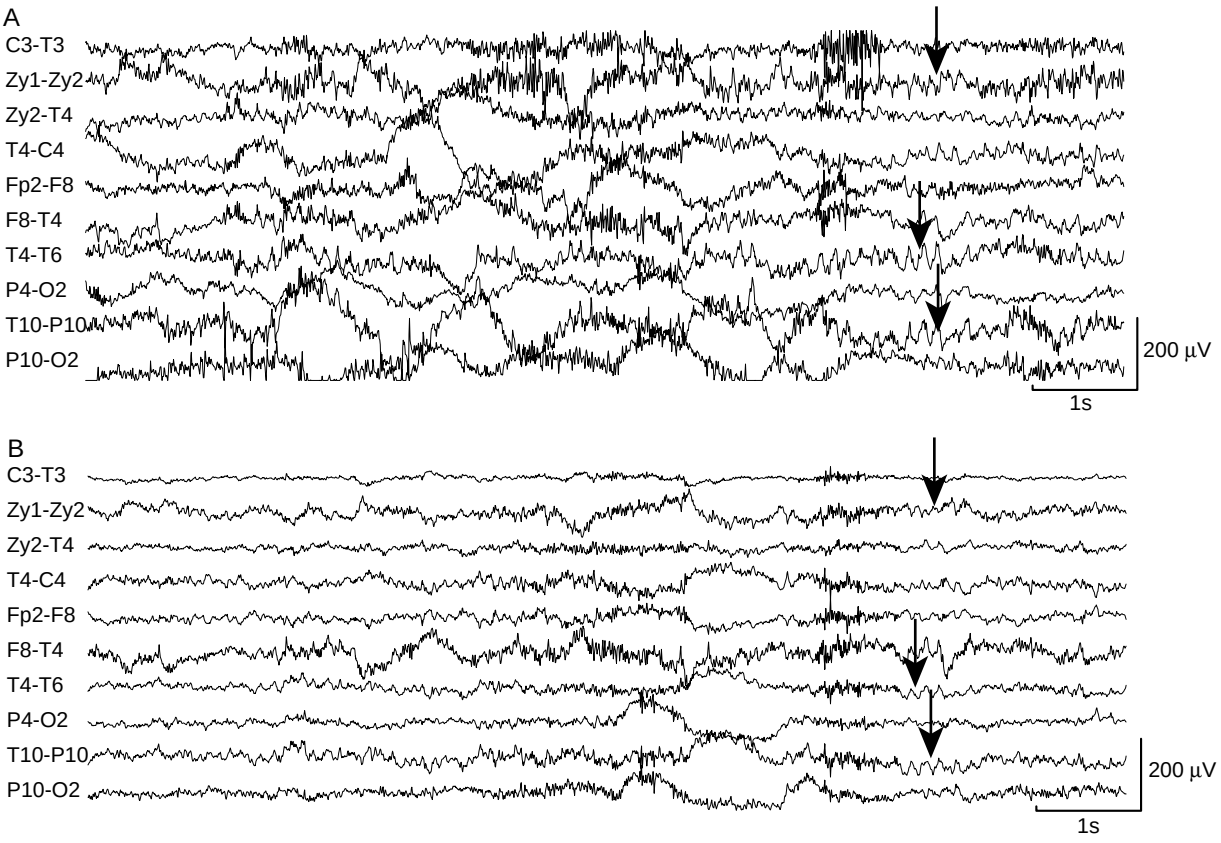

Fig. 10. (A) Seizure affected by movement artifacts and some EMG activity. (B) The automated system managed to attenuate the artifacts, but also removed cerebral activity. Arrows mark times where EEG activity in the original record has been greatly attenuated in the processed record.

Bayesian networks can offer a performance comparable or better than other state-of-the-art classifiers such as C4.5 decision trees (Friedman et al., 1997).

In many cases, it was unclear whether an epoch represented EEG activity or artifact. This can account for a lot of variability in the gold standard based on the reviewer's markings. In a study on EMG artifact detection in the EEG, van de Velde et al. evaluated the performance of an expert reviewer marking EMG artifacts on the same recordings twice (van de Velde et al., 1998). Using 1 s epochs, the reviewer correctly identified 82.6% of EMG epochs that were marked on a previous run with the same dataset. Also, 92.1% of non-EMG epochs were detected during the second run. In another study by the same group, two expert reviewers identified artifacts of various types in long-term EEG recordings, using 10 s epochs (van de Velde et al., 1999). On average, 76% of the artifacts marked by one expert were also marked by the other. For non-artifactual epochs, the average consensus was typically higher than 95%.

These measures of intra- and inter-expert variability provide a benchmark on the performance of the automated system. It successfully detected 82.4% of EEG epochs and 83.3% of artifactual epochs in the validation set. Sensitivity to artifacts is thus similar to the experts' performance. This success rate may be partly due to the fact that the analysis was performed on ICA components, where strong sources are separated into individual signals, rather than on raw EEG. On the other hand, the detection of EEG epochs was worse than the experts' performance. However, van de Velde et al. have attributed the high inter-expert consensus on EEG epochs to the low occurrence of artifacts (van de Velde et al., 1999). The prolonged EEG recordings used in their study contained lengthy periods of artifact-free data. This was not the case for the ictal EEG used in the current study, which tended to be heavily contaminated by artifacts because epileptic seizures are often accompanied by involuntary movements and automatisms.

4.3. Component classification

The area under the ROC curve for the number of EEG epochs determining whether to preserve or reject ICA components was 0.923, indicating that using a threshold would provide a good separation between the two types of components. It was crucial to preserve the EEG activity from the recording, hence the requirement for 90% sensitivity to EEG components in the training data. The threshold of 3.92, out of a maximum of 15 epochs per component, was consistent with the epoch classification accuracy of the system. A lower threshold would not be sufficient to detect significant EEG activity, since a few EEG epoch detections might be entirely due to the classification error rate.

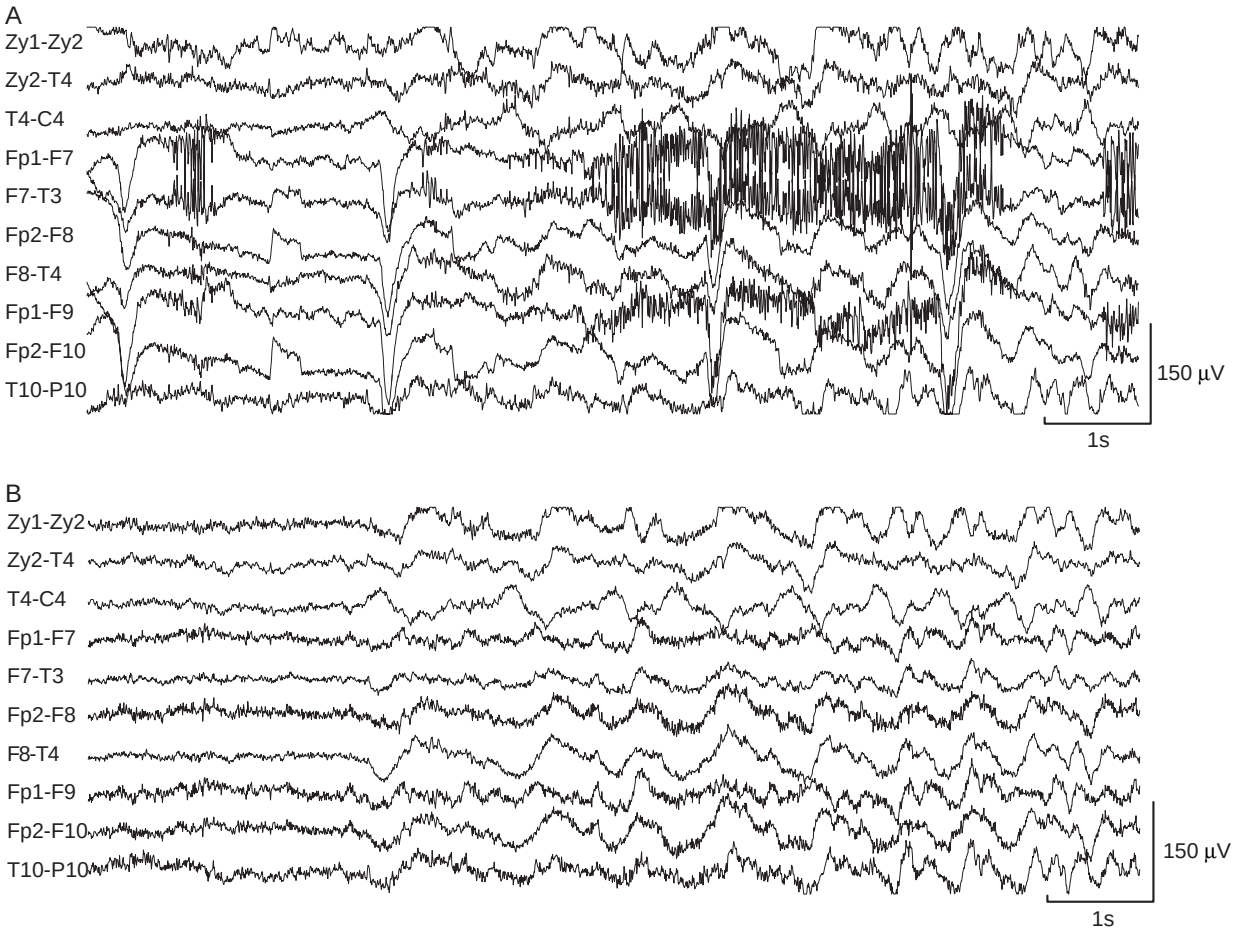

Fig. 11. (A) Seizure contaminated by numerous artifacts. EMG activity is visible in channels Fp1-F7, F7-T3, and Fp1-F9. Ocular artifacts are also present on channels Fp1-F7, F7-T3, Fp2-F8, F8-T4, Fp1-F9, and Fp2-F10. (B) After processing by the automated system, most of the artifacts are eliminated, while all EEG activity is preserved.

In the validation set, the identification of EEG components was performed with a sensitivity of 87.6% and specificity of 70.2%, which were only slightly worse than the inter-expert performance described above. A significant proportion of artifactual components can thus be removed by the automated system, while still preserving most of the EEG activity.

The two types of misclassifications (EEG components classified as artifact and vice-versa) occurred with similar types of components. In most cases, the components were a mixture of artifact and some minor EEG activity. Whether to preserve or reject the component depended on the subjective judgment of the reviewer, which suffered from some inherent variability. The error rate of the classifier can thus be partly attributed to these inconsistencies in the reviewer markings in the training data.

4.4. Analysis of reconstructed seizures

There are no absolute measures of the ease of interpretation of a seizure recording, so a subjective method had to be designed. This approach was similar to the one used by Urrestarazu et al. (Urrestarazu et al., 2004), who evaluated the quality of EEG reconstructed after removing visually selected artifactual components extracted by ICA. On the other hand, the current study used a completely automated system to select the appropriate components.

During the qualitative evaluation process by the reviewer, both the original and the processed records were examined simultaneously. This method was necessary to evaluate the preservation of EEG activity by the automated system. Seizures can exhibit a wide variety of EEG patterns, ranging from high-amplitude rhythms to more subtle discharges (Blume et al., 1984). There is consequently no clear measure of the amount of EEG activity, and any attenuation can thus only be recognized by directly comparing the original and processed signals.

The reviewer indicated that most seizures were contaminated by a significant amount of artifacts. This is typical of ictal EEG (Gotman, 1999), which is often accompanied by involuntary clinical symptoms that are responsible for some of the artifacts appearing on the EEG. The artifacts often complicate the seizure interpretation, especially if they are present at the time of the seizure onset. In this case, the

seizure records were thus likely to benefit greatly from the automated system of artifact removal. The system could be useful in removing doubts regarding the analysis of a seizure, confirming the interpretation from the original unprocessed record. The reconstructed EEG record could also help identify cerebral activity that might otherwise be difficult to notice in the original EEG. The automated system would thus be intended for seizures that are difficult to interpret due to a large number of artifacts obscuring the EEG.

The system provides an effective way of automatically removing several types of artifacts from ictal scalp EEG to facilitate seizure interpretation by clinicians. It is an advantageous alternative to digital filters, which are currently in common use in clinical applications. While filters can often eliminate a good portion of artifactual activity, their effectiveness is limited because of the overlap between the spectra of artifacts and seizure activity. The use of a highpass filter to eliminate movement or ocular artifacts would thus also attenuate EEG activity in the delta band. Lowpass filters have been used to remove EMG artifacts at high frequencies for which very little ictal EEG is present (Gotman et al., 1981), but the EMG spectrum has been shown to contaminate the EEG beta band as well (Goncharova et al., 2003). On the other hand, ICA methods have the ability to separate sources that overlap in the frequency domain. Nevertheless, digital filters could be used in conjunction with the automated system, which could further improve the quality of the EEG recording (Urrestarazu et al., 2004).

5. Conclusion

The main difficulty with ICA-based methods for artifact removal in ictal EEG is the tedious visual selection of artifactual components. The proposed system can automate this process, thus allowing this approach to be used in a practical way in a clinical setting. The use of a TAN Bayesian framework allowed a large number of features to be used in the classification task. This yielded a classifier with a performance that was only slightly worse than the errors that would be expected from human expert variability. Therefore, this system is expected to improve the interpretability of seizures recorded on scalp EEG by removing a significant portion of artifacts obscuring the EEG activity.

Acknowledgements

This project was supported by the Canadian Institutes of Health Research grant MOP-10189 and the National Engineering Science and Research Council scholarship CGSM.

References

Barbati G, Porcaro C, Zappasodi F, Rossini PM, Tecchio F. Optimization of an independent component analysis approach for artifact identification and removal in magnetoencephalographic signals. Clin Neurophysiol 2004;115:1220–32.

Blume WT, Young GB, Lemieux JF. EEG morphology of partial epileptic seizures. Electroencephalogr Clin Neurophysiol 1984;57:295–302.

Cormen TH, Leiserson CE, Rivest RL. Introduction to algorithms. Cambridge, MA: MIT Press; 1990.

Delorme A, Makeig S. EEGLAB: an open source toolbox for analysis of single-trial EEG dynamics including independent component analysis. J Neurosci Methods 2004;134:9–21.

Delorme A, Makeig S, Sejnowski T. Automatic artifact rejection for EEG data using high-order statistics and independent component analysis. In: Proceedings of third international independent component analysis and blind source decomposition conference, San Diego, CA; 2001. p. 457–62.

Delsanto S, Lamberti F, Montrucchio B. Automatic ocular artifact rejection based on independent component analysis and eyeblink detection. In: Proceedings of the first international IEEE EMBS conference on neural engineering, Capri Island, Italy; 2003. p. 309–12.

Fayyad U, Irani K. Multi-interval discretization of continuous-valued attributes for classification learning. In: Proceedings of 13th international joint conference on artificial intelligence; 1993. p. 1022–29.

Flanagan D, Agarwal R, Wang YH, Gotman J. Improvement in the performance of automated spike detection using dipole source features for artefact rejection. Clin Neurophysiol 2003;114:38–49.

Friedman N, Geiger D, Goldszmidt M. Bayesian network classifiers. Mach Learn 1997;29:131–63.

Goncharova II, McFarland DJ, Vaughan TM, Wolpaw JR. EMG contamination of EEG: spectral and topographical characteristics. Clin Neurophysiol 2003;114:1580–93.

Gotman J. Automatic detection of seizures and spikes. J Clin Neurophysiol 1999;16:130–40.

Gotman J, Ives JR, Gloor P. Frequency content of EEG and EMG at seizure onset: possibility of removal of EMG artefact by digital filtering. Electroencephalogr Clin Neurophysiol 1981;52:626–39.

Gratton G, Coles MG, Donchin E. A new method for off-line removal of ocular artifact. Electroencephalogr Clin Neurophysiol 1983;55:468–84.

Grewal S, Gotman J. An automatic warning system for epileptic seizures recorded on intracerebral EEGs. Clin Neurophysiol 2005;116:2460–72.

Hyvarinen A, Oja E. A fast fixed-point algorithm for independent component analysis. Neural Comput 1997;9:1483–92.

Hyvarinen A, Oja E. Independent component analysis: algorithms and applications. Neural Netw 2000;13:411–30.

Hyvarinen A, Karhunen J, Oja E. Independent component analysis. New York: Wiley; 2001.

Ille N, Berg P, Scherg M. Artifact correction of the ongoing EEG using spatial filters based on artifact and brain signal topographies. J Clin Neurophysiol 2002;19:113–24.

Inouye T, Shinosaki K, Sakamoto H, Toi S, Ukai S, Iyama A, Katsuda Y, Hirano M. Quantification of EEG irregularity by use of the entropy of the power spectrum. Electroencephalogr Clin Neurophysiol 1991;79:204–10.

Iwasaki M, Kellinghaus C, Alexopoulos AV, Burgess RC, Kumar AN, Han YH, Luders HO, Leigh RJ. Effects of eyelid closure, blinks, and eye movements on the electroencephalogram. Clin Neurophysiol 2005;116:878–85.

James CJ, Gibson OJ. Temporally constrained ICA: an application to artifact rejection in electromagnetic brain signal analysis. IEEE Trans Biomed Eng 2003;50:1108–16.

Jung TP, Makeig S, Lee TW, McKeown MJ, Brown G, Bell AJ, Sejnowski TJ. Independent component analysis of biomedical signals. In: The second int'l workshop on independent component analysis and signal separation; 2000. p. 633–44.

Kobayashi K, Merlet I, Gotman J. Separation of spikes from background by independent component analysis with dipole modeling and comparison to intracranial recording. Clin Neurophysiol 2001;112:405–13.

Lagerlund TD, Sharbrough FW, Busacker NE. Spatial filtering of multichannel electroencephalographic recordings through principal component analysis by singular value decomposition. J Clin Neurophysiol 1997;14:73–82.

Lee TW, Girolami M, Sejnowski TJ. Independent component analysis using an extended infomax algorithm for mixed sub-gaussian and super-gaussian sources. Neural Comput 1999;11:417–41.

Lu W, Rajapakse JC. Approach and applications of constrained ICA. IEEE Trans Neural Netw 2005;16:203–12.

Makeig S, Bell AJ, Jung TP, Sejnowski TJ. Independent component analysis of electroencephalographic data. In: Advances in neural information processing systems, vol. 8; 1996a. p. 145–51.

Makeig S, Jung TP, Ghahremani D, Sejnowski TJ. Independent component analysis of simulated ERP data. San Diego, CA: Institute for Neural Computation, University of California; 1996b. Report no. INC-9606.

Metz CE. Basic principles of ROC analysis. Semin Nucl Med 1978;8: 283–98.

Nam H, Yim TG, Han SK, Oh JB, Lee SK. Independent component analysis of ictal EEG in medial temporal lobe epilepsy. Epilepsia 2002;43: 160–4.

Niedermeyer E, Lopes da Silva F. Electroencephalography: basic principles, clinical applications, and related fields. 5th ed. Philadelphia, PA: Lippincott/Williams & Wilkins; 2005.

Park S, Lee H, Choi S. ICA + OPCA for artifact-robust classification of EEG data. In: Neural networks for signal processing, 2003. NNSP'03. 2003 IEEE 13th workshop on 2003. p. 585–94.

Romero S, Mananas MA, Riba J, Morte A, Gimenez S, Clos S, Barbanoj MJ. Evaluation of an automatic ocular filtering method for awake spontaneous EEG signals based on independent component analysis. In: Engineering in medicine and biology society, 2004. EMBC 2004. Conference proceedings. 26th annual international conference of the 2004. p. 925–28.

Saab ME, Gotman J. A system to detect the onset of epileptic seizures in scalp EEG. Clin Neurophysiol 2005;116:427–42.

Srinivasan R, Nunez PL, Silberstein RB. Spatial filtering and neocortical dynamics: estimates of EEG coherence. IEEE Trans Biomed Eng 1998; 45:814–26.

Swets JA. Measuring the accuracy of diagnostic systems. Science 1988; 240:1285–93.

Urrestarazu E, Iriarte J, Alegre M, Valencia M, Viteri C, Artieda J. Independent component analysis removing artifacts in ictal recordings. Epilepsia 2004;45:1071–8.

van de Velde M, van Erp G, Cluitmans PJ. Detection of muscle artefact in the normal human awake EEG. Electroencephalogr Clin Neurophysiol 1998;107:149–58.

van de Velde M, Ghosh IR, Cluitmans PJ. Context related artefact detection in prolonged EEG recordings. Comput Methods Programs Biomed 1999;60:183–96.

Whitton JL, Lue F, Moldofsky H. A spectral method for removing eye movement artifacts from the EEG. Electroencephalogr Clin Neurophysiol 1978;44:735–41.